

Charge separation in photosystem II core complexes induced by 690–730 nm excitation at 1.7 K

Joseph L. Hughes^a, Paul Smith^b, Ron Pace^b, Elmars Krausz^{a,*}

^a *Research School of Chemistry, Australian National University 0200 Canberra, Australia*

^b *Faculty of Science, Australian National University 0200 Canberra, Australia*

Received 30 March 2006; received in revised form 1 May 2006; accepted 22 May 2006

Available online 2 June 2006

Abstract

The illumination of oxygen-evolving PSII core complexes at very low temperatures in spectral regions not expected to excite P680 leads to charge separation in a majority of centers. The fraction of centers photoconverted as a function of the number of absorbed photons per PSII core is determined by quantification of electrochromic shifts on Pheo_{D1}. These shifts arise from the formation of metastable plastoquinone anion (Q_A^{•−}) configurations. Spectra of concentrated samples identify absorption in the 700–730 nm range. This is well beyond absorption attributable to CP47. Spectra in the 690–730 nm region can be described by the ‘trap’ CP47 absorption at 689 nm, with dipole strength of ~1 chlorophyll *a* (chl *a*), partially overlapping a broader feature near 705 nm with a dipole strength of ~0.15 chl *a*. This absorption strength in the 700–730 nm region falls by 40% in the photoconverted configuration. Quantum efficiencies of photoconversion following illumination in the 690–700 nm region are similar to those obtained with green illumination but fall significantly in the 700–730 nm range. Two possible assignments of the long-wavelength absorption are considered. Firstly, as a low intensity component of strongly exciton-coupled reaction center chlorin excitations and secondly as a nominally ‘dark’ charge-transfer excitation of the ‘special pair’ P_{D1}–P_{D2}. The opportunities offered by these observations towards the understanding of the nature of P680 and PSII fluorescence are discussed. © 2006 Elsevier B.V. All rights reserved.

Keywords: Charge transfer; Reaction center; Exciton coupling; Photoconversion; Quantum efficiency

1. Introduction

The unique capacity of photosystem II (PSII) to photo-oxidize water with visible light identifies this enzyme as the engine-room of life on Earth. PSII is the source of virtually all bio-energetic electrons in nature. Despite decades of sustained effort, no widely accepted description of the photo-active pigment/protein assembly of PSII (P680) has emerged. Recent X-ray data have confirmed strong structural analogies of the PSII reaction center to that of the Bacterial Reaction Center (BRC), the latter assemblies being possible antecedents of the former.

The *minimal* photosynthetic assembly retaining oxygen-evolving capacity [1] is a PSII core complex, composite of the D1/D2/cytb₅₅₉ reaction center proteins, CP47 and CP43 proximal antennae, Mn-stabilizing proteins, and other ancillary proteins. PSII core complexes of thermophilic cyanobacteria have

been successfully crystallized leading to medium resolution structural data [2–6]. Detergent solubilization of PSII core complexes leads to isolated D1/D2/cytb₅₅₉ reaction centers [7]. These assemblies do not bind a secondary acceptor, cannot evolve oxygen, and show efficient and reversible primary charge separation, forming P680⁺–Pheo^{•−}. In contrast to BRCs they have not been purified to the level needed for successful crystallization.

Reaction center preparations of PSII continue to be extensively studied, most recently using Stark [8] and ultra-fast spectroscopic techniques [9–12]. These preparations have been used in a very wide range of experiments. The results of these experiments have formed the basis for a range of models for P680 [13–16]. However it has been suggested [17–21] that this assembly is not fully representative of the reaction center in intact PSII cores. We have, on the basis of comparative studies of isolated subunits and cores using a range of low temperature spectroscopies [1,18–23], suggested that there is substantial inhomogeneous broadening in the isolated reaction centers and that their properties are not fully representative of the charge separating assembly in the native system.

* Corresponding author. Tel.: +61 2 6125 3577; fax: +61 2 6125 0750.

E-mail address: krausz@rsc.anu.edu.au (E. Krausz).

Core complexes have not been as extensively studied by optical spectroscopies although they exhibit significantly better spectral detail at low temperatures [1,21–23]. PSII core complexes show variability in this structure when prepared from different organisms [21]. A key difficulty in the design of experiments and subsequent analysis of the optical spectra of cores is that the chlorophyll and β -carotene pigments in CP43 and CP47 dominate the spectra. The reaction center absorptions overlap those of the proximal light-harvesting assemblies CP43 and CP47 and the resulting spectral congestion makes unambiguous identification and assignment of excitations difficult.

Whereas low temperature excitation of reaction center preparations leads to a short-lived (primary) charge-separated state, illumination of core complexes at 1.7 K gives rise to very long-lived [22] charge-separated configurations. The latter are associated with the formation of a stable plastoquinone anion (Q_A^-) together with a partnering secondary donor, which is often an oxidized β -carotene. The fraction of PSII that is photoconverted to a charge-stabilized configuration can be reproducibly and quantitatively determined by monitoring the absorption spectrum before and after illumination [22,24]. The electrochromic shift of the D1 pheophytin *a* (Pheo_{D1}) pigment can be monitored either by changes in the Q_x band near 545 nm or in the corresponding Q_y band at 685 nm. These wavelengths are for spinach cores and although they are distinctly different for other organisms, the same phenomenology is exhibited [21]. The Q_x shift is known as the ‘C550’ signal and was originally observed via illumination of chloroplast preparations at 77 K [25,26].

Excitation of PSII cores with narrowband (laser) radiation at wavelengths longer than 676 nm was found [23] to lead to remarkably efficient spectral hole-burning (SHB). When the PSII sample was initially poised in the dark-adapted (Q_A) state, efficient SHB was accompanied by the characteristic electrochromic shifts on Q_y and Q_x of Pheo_{D1}, which are unambiguous signatures of charge separation in PSII.

The extraordinarily high efficiency of hole-burning activity was attributed to activation of P680 (with subsequent charge separation) following relatively *slow* excitation transfer from CP43 and CP47 ‘linker’ chlorophylls to the reaction center [23,27]. Confirmation of this mechanism is provided by the observation [28] that spontaneous spectral hole-filling precisely tracks charge recombination of Q_A^- with the secondary donor.

The analysis of the SHB data [27] has led to a more complete understanding [29] of the complex characteristics of the temperature dependent emission spectra of PSII. The emission of PSII at low temperatures arises from subsets of CP43 and CP47 ‘linker’ pigments from within their inhomogeneous distributions. A similar conclusion with respect to CP43 ‘linker’ emission was later reached by Andrizhiyevskaya et al. [30] from an analysis of the temperature dependent emission spectra taken at different excitation wavelengths of PSII cores prepared from the cyanobacterium *Synechocystis* PCC 6803 and PSII core subunits prepared from spinach.

Our SHB work [23] provided the first evidence that efficient charge-separation in PSII could be induced, in the absence of significant thermal activation, with excitation wavelength well

beyond 680 nm. The possibility of thermal activation of the sample by the exciting light could be excluded as these experiments were performed at extremely low temperatures (1.7 K) and at low laser power-densities.

The strong SHB occurring in the 680–700 nm region when using narrowband excitation introduces difficulties in quantifying yields of Q_A^- formation. This is because the absorbance of the sample at the laser wavelength changes dramatically upon laser irradiation, due to the highly efficient SHB process induced. We have shown [24,29] that hole-burning can be largely circumvented by using broadband radiation from a monochromator/lamp system ($6\text{--}8\ \mu\text{W}/\text{cm}^2$, bandwidth 2.3 nm) to illuminate samples. With 2.3 nm bandwidth excitation, the SHB photoproduct falls mostly within the excitation bandwidth. Our initial report [24] established that substantial photoconversion of a PSII core sample to the Q_A^- configuration could be achieved with very low power density 2.3 nm bandwidth radiation with wavelengths as long as 700 nm.

In this paper we report charge separation in PSII cores immersed in superfluid helium at 1.7 K, as induced by illumination in the 690–730 nm range. Data are also provided for green illumination, the radiation most often used to photoconvert PSII samples. The fraction of centers undergoing primary charge separation and subsequent formation of the metastable Q_A^- configuration is quantified by electrochromic shifts in absorption spectra. High sensitivity absorption spectra taken of concentrated samples serve to identify the feature in the extreme red region that leads to the observed photo-induced charge separation. Quantification of the absorbance of PSII core samples in the 700–750 nm range in turn allows the extent of photoconversion to be mapped as a function of the absorbed number of photons per PSII.

2. Materials and methods

2.1. Biochemical samples and optical spectrometer

PSII core complexes with an oxygen-evolving activity of $3400\text{--}4000\ \mu\text{mol}$ of O_2 (mg of chl)⁻¹ h⁻¹ were isolated from spinach as previously described [1]. In order to minimize light scattering of the optical sample, a factor critical in identifying weak broad absorption in the red, a thin (200- μm pathlength and 12-mm diameter) quartz cell assembly was utilized with concentrated PSII core material (1–5 mg(chl *a*)/mL). The cyroprotectant used was 1:1 ethylene glycol/glycerol and its volume fraction adjusted to 40%. The sample was cooled to 4 K over a period of ~ 40 s [1,22,23].

A new sample was prepared for each illumination fluence dependence experiment. This avoided any effects due to degradation of the sample. Samples were dark-adapted for 5 min at 290 K, poisoning the sample in the $S_1(Q_A)$ configuration [22]. The laboratory-designed spectrometer that we used has been previously described [1,22,23]. The peak optical density of samples in the chlorophyll Q_y region ranged from ~ 2 to 3 for illuminations at wavelengths in the range 680–700 nm and $\sim 3\text{--}7$ for illuminations at wavelengths longer than 700 nm. All illuminations and measurements were performed with the sample immersed in superfluid helium at 1.7 K. There were no measurable spectral changes induced by the actinic light of the spectrometer.

2.2. Illumination sources

A number of illumination sources were utilized. For green-light illumination, light from a 150 W halogen lamp was passed through a 10 cm water bath and a green filter stack and then focussed at the sample. The maximum light

intensity at the focus was 5 mW/cm^2 , peaking at 540 nm and having a FWHM of $\sim 50 \text{ nm}$. The spectral profile of the lamp/filter system was measured, allowing the total number of photons absorbed in the sample for a given illumination period to be determined. Alternatively, 514 nm radiation from an Ar^+ laser was defocused and attenuated to a similar power density. The optical density of the samples in the region of green-light excitation was less than 0.1–0.4 ensuring uniform excitation through the optical path of the sample cell.

In the 680–700 nm region, a Spex 0.25-m double monochromator/250-W halogen lamp system operating with 1-mm slit widths was used. Light from the monochromator was further passed through a 630-nm filter before illuminating the sample. This system had a spectral width of 2.3 nm and the output power ($6\text{--}8 \mu\text{W/cm}^2$) was calibrated against a silicon diode of known sensitivity.

In the 695–715 nm range, a Spectraphysics 375 dye laser operating with DCM dye and 3-plate birefringent filter, pumped by a Spectraphysics model 175 Ar^+ laser was utilized. This system had a linewidth of $\sim 0.05 \text{ nm}$. In the 710–800 nm region, a Schwartz Ti:Sapphire laser with linewidth of $< 0.001 \text{ nm}$ was utilized. Laser light was used at far field (see below). This ensured a uniform power density across the (central) portion of the beam used for illumination.

2.3. Light purity

Before passage to the sample, the output of either the dye or Ti:Sapphire laser was reflected from a Littrow prism and propagated $\sim 11 \text{ m}$. This procedure effectively isolated any background fluorescence from the tuneable laser light. The beam was then passed through a polarization scrambler and finally a 665 nm long pass filter, which served to remove residual ambient and Ar^+ laser pump light.

Control (null) illumination experiments were performed with the tuneable lasers excited at full Ar^+ pump power, and therefore fluorescing maximally, but with laser action inhibited by small adjustment of the output coupler of the laser cavity. Under these conditions, no photoconversion of the samples was seen even after a 15 min test ‘illumination’. Consequently all photoconversion reported was induced solely by light at the specified wavelength.

3. Results

3.1. Illumination-induced spectral changes

Fig. 1 illustrates the ‘C550’ shift of the Q_x transition of Pheo_{D1} as measured in a PSII core sample at 1.7 K. The shape of the difference spectrum did not change with fractional photo-conversion of the sample or wavelength of illumination and thus the difference amplitude can be reliably used to monitor the fraction of the sample in which Q_A has been photo-reduced.

Calibration of the absorption difference amplitude (Fig. 1) at full conversion of the sample to the Q_A^- configuration was determined by a comparison of the saturating amplitude of the ‘C550’ signal obtained by sustained photo-reduction compared to the corresponding signal obtained by chemical reduction of Q_A . Additionally, the same amplitude of ‘C550’ signal was obtained after an $S_1(Q_A)$ sample was illuminated at 260 K with green light and then rapidly frozen. This protocol is known [1] to poise the system in the $S_2(Q_A)$ (EPR multiline) configuration in more than 90% of centers. These checks establish that saturating illumination with green light (see Materials and methods) at 1.7 K is effective in converting $\sim 95 \pm 5\%$ of the Q_A to the metastable $S_1(Q_A^-)$ configuration.

Fig. 2 presents an absorption spectrum of PSII cores in the red, extending to 740 nm. The minimal scattering in our optical samples is evident once noting that no baseline corrections have been made to the spectra. Although illumination-induced electrochromism absorption changes in the Q_y region have am-

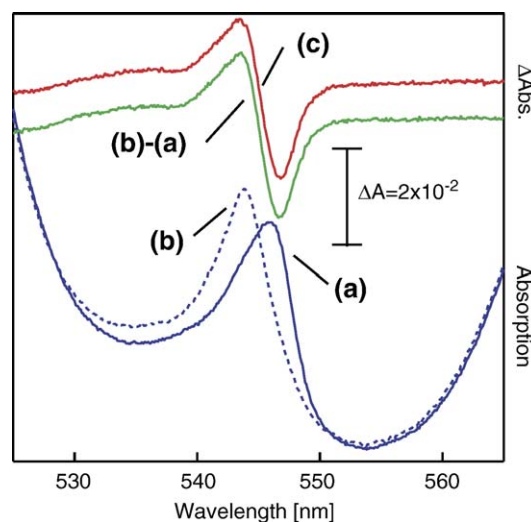


Fig. 1. The pheophytin Q_x absorption region of a spinach PSII core complex at 1.7 K. Trace (a) is before and trace (b) after green illumination leading to $> 95\%$ Q_A reduction. The difference spectrum (b)–(a) is the ‘C550’ signal attributed to an electrochromic shift of the Pheo_{D1} Q_x transition. Trace (c) is the corresponding electrochromic shift resulting from $\sim 1 \text{ J/cm}^2$ absorbed fluence at 720 nm, leading to 45% Q_A reduction in a sample $\sim 2\times$ more concentrated than used for the green illumination experiment.

plitudes $\sim 10\times$ larger than those seen in the Q_x region, the fractional changes relative to the absorption in Q_y are smaller. We have assigned [21,22] the prominent lowest-energy derivative feature centered at 685 nm as an electrochromic blue shift on Pheo_{D1} associated with Q_A^- formation.

The amplitudes of the ‘C550’ shift and the 685 nm shift were found to track each other quantitatively. Either spectral feature can thus be used to determine Q_A^- formation. In samples with high optical density in the Q_y region, i.e. in the concentrated samples used to investigate the photoconversion in the extreme red where absorbances are low, monitoring the Q_x feature is more effective in quantifying Q_A^- formation. This is because optical densities at 685 nm are > 2.5 , which leads to poor signal-to-noise ratios and stray light artefacts.

Absorption and illumination-induced absorption changes beyond 680 nm are presented in Fig. 3. These spectra were taken on a sample that was $\sim 2\times$ more concentrated than that used for Fig. 2 and on a $\sim 10\times$ more sensitive absorbance scale. Most notable is that there is absorption in the 700–730 nm region. There are also illumination-induced absorption changes in this region. These changes are directly proportional to the extent of Q_A^- formation [28,31]. The spectral profile of this illumination-induced change is also independent of the wavelength of excitation [28]. The absorption change seen in the 700–730 nm range, which corresponds to a 40% decrease in absorption for 100% Q_A^- formation, has the same spectral profile as the absorption in this region. This correspondence suggests that the absorption in this region is associated with a major fraction of PSII cores and not with a minor impurity or a small fraction of the sample consisting of degraded or modified PSII cores.

Absorption in the 700–730 nm region is difficult to detect in dilute samples. However, we have found that an equivalent photoconversion of dilute samples occurs with 700–730 nm

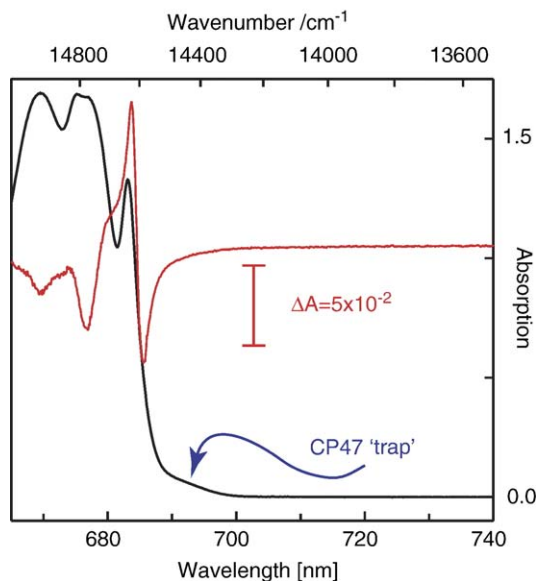


Fig. 2. Absorption spectrum of PSII cores at 1.7 K (lower trace) in the 665–740 nm region. No baseline corrections have been made. The upper curve is the after-minus-before green light illumination spectrum. The strong derivative feature present in the difference spectrum at 685 nm is a blue shift on the Pheo_{D1} Q_y band [22] and the CP47 ‘trap’ absorption is indicated.

illumination. This, along with the fact that all our samples are prepared with a detergent concentration of 0.3 mg/mL *n*-dodecyl β -D-maltoside [1] excludes the possibility that absorption in the 700–730 nm region is due to aggregates.

3.2. Wavelength dependence of photoconversion yields

The yield of Q_A⁻ formation as a function of absorbed fluence, using green light illumination is presented in Fig. 4. At the

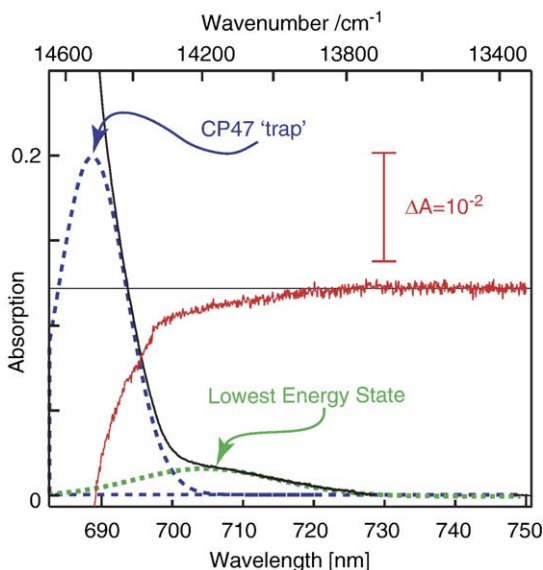


Fig. 3. Absorption (lower trace) and electrochromism difference-spectrum (upper trace) as for Fig. 2, taken in the 680–750 nm regions utilizing a PSII sample with OD \sim 3 at 670 nm. Dashed lines are obtained from a Gaussian least-squared fit of the absorbance (see text). The sum of the two dashed curves quantitatively reproduces the observed absorption spectrum.

lowest fractional conversion, quantum efficiencies (QEs) of photoconversion are high. A 50% overall conversion of the sample occurs with an average QE of \sim 0.1, in agreement with our previous estimates of QEs based on SHB and other measurements [22,23]. The data in Fig. 4 are also entirely consistent with a 10–15% conversion observed [25] for cryogenic PSII samples initially poised in the Q_A state and converted to a stable Q_A⁻ configuration by a brief ‘saturating’ light flash configured to photo-excite each center only once. Although the photo-efficiency of (transient) Q_A⁻ formation is far higher and may approach that seen for PSII at ambient temperatures, only a fraction of the charge separated configuration is stable for > 60 s and is relevant to our measurements.

A 10^2 – 10^3 greater absorbed fluence is required to achieve complete conversion of a sample to a stable Q_A⁻ configuration. We have observed entirely analogous photoconversion yield behaviors in membrane-bound PSII particles (BBYs) and thylakoids prepared from plants (spinach), as well as cyanobacterial PSII cores (*Synechocystis* PCC 6803). PSII core preparations with significantly lower oxygen-evolving activities also show an analogous behavior. The yield characteristic appears to be intrinsic to PSII rather than being related to the activity of a PSII preparation or its level of integrity.

Fig. 5 presents a set of photoconversion data with excitation over the wavelength range from 690 nm to 728 nm. Data are presented in terms of fractional conversion of the sample versus absorbed photons per PSII core particle. Data from green-light illumination-induced photoconversion are also provided as a reference. Also presented on the graph are a family of theoretical conversion curves. These curves assume all PSII cores in the sample have the same QE using a first order rate equation. Curves are shown for each decade of QE from 1 to 10^{-4} . Clearly, no single QE can account for the experimental data.

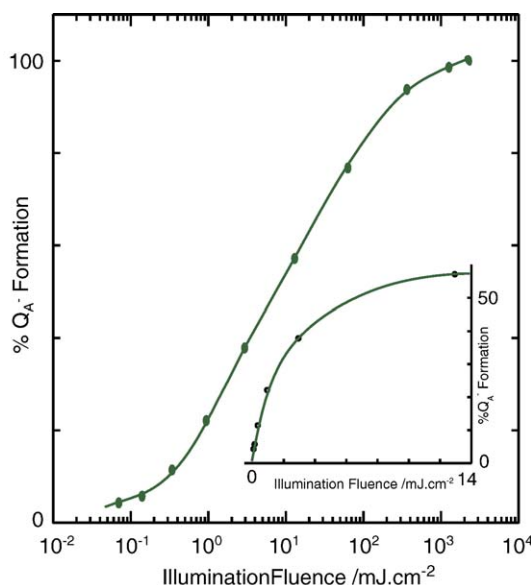


Fig. 4. The absorbed fluence dependence of Q_A⁻ formation at 1.7 K in PSII cores isolated from spinach for green-light illumination (see Materials and methods). The solid lines are provided as a guide for the eye.

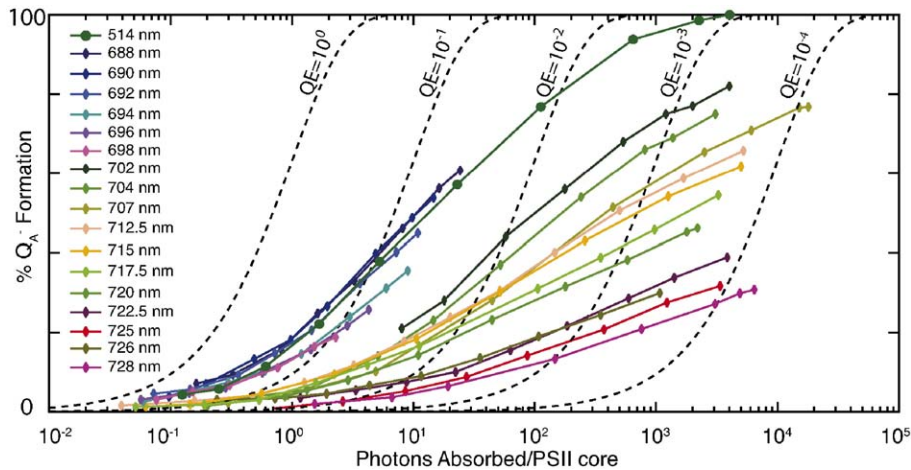


Fig. 5. Photoconversion of PSII cores at 1.7 K, as monitored by Q_A^- formation at 1.7 K as a function the number of photons absorbed per PSII at the wavelengths indicated. For the 690–704 nm region where hole-burning occurs, illuminations were performed with a monochromator/lamp illumination source (see Materials and methods) and laser illumination (see Materials and methods) was used beyond 704 nm. Dotted lines are theoretical conversion curves for quantum efficiencies (QEs) indicated (see text).

Attempts to model the observed photoconversion yield with a Gaussian or polynomial distribution of QEs were not successful. A more successful approach was to allow for more than 2 distinct QEs. The assumption of 3 distinct QEs led to a reasonable fit. The QEs were 0.7, 0.05 and 0.003 all with comparable amplitude contribution in the fit. Significant correlations were seen between fit parameters and a detailed analysis of this QE distribution is beyond the scope of this paper.

Conversion efficiencies with illumination in the 690–700 nm range (with 2.3 nm bandwidth) show yields of Q_A^- formation comparable to that seen with green light. Saturating absorbed fluences in this wavelength range could not be achieved due to the low power of the lamp-based illumination system that was utilized (Materials and methods). As mentioned previously, broadband light was used in the 690–700 nm region to limit the impact of strong SHB that occurs with narrowband (laser) excitation in this region.

SHB is not evident in the 700–730 nm region [28]. Thus, laser sources can be utilized to illuminate samples and the decrease in absorbance in this region upon Q_A^- formation can be easily accounted for. The increased power of laser sources helps to compensate for the very low absorbance (< 0.02) in the range beyond 700 nm. However, the highest *absorbed* power density utilized remains low (2–5 mW/cm²) and comparable to that used with green illumination (of more dilute samples). The data in Fig. 5 shows that an illumination equivalent to exciting each center $\sim 10^3$ times at 707 nm (~ 20 min 160 mW/cm² *incident* power) leads to $\sim 80\%$ conversion of the sample to the Q_A^- state. Even with this level of absorbed fluence, saturation has not been achieved (Fig. 5). Longer illumination periods are inconclusive due to a partial decay of the metastable Q_A^- configuration on the ~ 20 min timescale. Higher laser powers were not available.

The number of absorbed photons required to photoconvert the first 20% of a dark-adapted PSII sample in the $S_1(Q_A)$ configuration increases very significantly as illumination wavelengths longer than 700 nm are used. The increase is a factor of

~ 10 at 707 nm and $\sim 10^3$ at 725 nm. Excitation at 726 nm appears to be slightly more efficient than at 725 nm. We attribute this anomaly to our inability to accurately determine the magnitude of the tailing absorption at the very longest wavelengths in some samples. We have found that illumination beyond 730 nm leads to minimal photoconversion. For example, sustained (~ 10 min) illumination of samples with 450 mW/cm² of 750 nm light leads to no quantifiable Q_A^- formation (i.e. $< 3\%$).

4. Discussion

4.1. Charge separation as monitored via Q_A^- formation

Our experiments monitor metastable secondary acceptor reduction (Q_A^- formation) via electrochromic shifts of Pheo_{D1}. We have identified significant variations in the QE of Q_A^- formation as a function of both the absorbed fluence and the excitation wavelength. Whether these effects are determined by variations in the *primary* charge separation processes forming $P680^+ - \text{Pheo}_{D1}^-$ or by factors in the subsequent processes of secondary acceptor reduction and donor oxidation cannot be immediately determined from our data. As previously mentioned, we have green-illumination data (not shown) similar to that in Fig. 2 for a range of PSII samples and from these data the dispersion of QEs appears to be intrinsic to PSII. We note that there have been analyses of photon echoes [11] and SHB [32] in D1/D2/cyt_{b559} preparations pointing to a highly dispersive primary charge separation process. This allows for the possibility that the wide variation of formation efficiencies of Q_A^- may arise from variations in primary charge separation processes.

The ‘C550’ shift is a robust and quantitative indicator that charge separation has occurred in PSII *and* that metastable Q_A^- formation was successful. The Q_x difference-spectra induced by illuminations at either 540 or 705 nm (Fig. 1) are identical, indicating that the same photoconversion process has been induced as far as its influence on Pheo_{D1}. The blue shift

centered at 685 nm in spinach scales with the Q_x shift for all wavelengths of excitation. However, other illumination-induced changes in the 650–680 nm region [21,22] are variable, even between BBYs and PSII cores both prepared from spinach. The illumination-induced spectral changes seen in this region for *Synechococcus elongatus* (our unpublished results and Hillman et al. [33]), for example, are distinctly different to those seen for spinach or *Synechocystis* PCC 6803 [22]. In each organism, we have assigned the lowest energy derivative feature as due to an electrochromic shift of Q_y on Pheo_{D1}.

There is a range of low-temperature secondary donors in PSII that can be oxidized upon metastable Q_A^- formation. These donors include Chl_Z, β -carotene, Cyt_{b559}, Tyr_Z and Tyr_D [34–38]. In our core samples, Cyt_{b559} is fully oxidized and is not available as a donor. The degree of Chl_Z oxidation induced by a saturating green illumination at 1.7 K is somewhat variable and Chl_Z acts as the secondary donor in 10–50% of PSII centers in our core samples. This is quantified by integration of the absorption difference-spectra in the 650–700 nm region. We have identified β -carotene as a significant donor in our samples [22]. Using the molar extinction values for the β -carotene radical cation [37,39] or the fractional bleach in the 450–500 nm range while knowing [1,22] the number of β -carotenes per PSII center in our core samples, we are able to quantify that ~20–30% of PSII utilize β -carotene as a secondary donor.

4.2. Characterization of the low energy states in PSII cores

Systematic SHB and circular dichroism (CD) measurements [20,28,31] have established that there is no significant contribution to the absorption in the 690–730 nm region from either PSI or LHCI-730 in our (plant) PSII cores samples. The 700–730 nm region was shown to have no measurable CD activity but had the characteristic (+) B term Magnetic CD signal of a Q_y transition in chlorophyll or pheophytin [20,31].

We have previously assigned the prominent feature at 683.5 nm in Fig. 2 to the quasi-degeneracy (in spinach PSII) of CP43 and reaction center (P680) absorptions. This accidental degeneracy is lifted in *Synechocystis* PCC 6803 cyanobacterial PSII [21]. The linewidth of the 685 nm absorption assigned to Pheo_{D1}, via integration of the electrochromic signature, is ~2.5 nm (70 cm⁻¹) [22]. Absorption in the 690–700 nm region is dominated by the well-known CP47 ‘trap’ feature having a width of ~10 nm. This band is the lowest energy absorption in CP47 and has an almost identical spectrum in isolated CP47 subunit preparations. In both cores and in isolated CP47, the band exhibits a (+) CD spectrum. This CD activity helps to quantify the position and lineshape of the absorption.

The lack of any SHB or CD activity in the 700–730 nm region each confirms that absorption in this region does not arise from CP47. CP47 subunits do not show absorption beyond 704 nm in PSII cores [28]. The lack of SHB in the 705–730 nm region in PSII cores [28] helps establish that this absorption is dominantly homogeneously broadened. By contrast, strong SHB and fluorescence line narrowing (FLN) is seen for the CP47 trap state, as present in either isolated CP47 subunits or as part of intact PSII [23,27,29,40,41]. Thus the CP47 state is

strongly inhomogeneously broadened, in contrast to any state in the 700–730 nm region.

The absorption in the 690–730 nm spectral region (Fig. 3) can be fitted to the sum of Gaussians centered at 688.5±0.5 nm (240±10 cm⁻¹ FWHM) and 704.8±0.5 nm (475±50 cm⁻¹ FWHM) respectively. The 688.5 nm CP47 feature has an area corresponding to 1.0±0.05 chl *a* and the low energy band an area corresponding to 0.15±0.05 chl *a* (when the sample is poised in the Q_A configuration). The area, position and width of the CP47 feature in our fit are entirely consistent with linear dichroism [42] and CD data (our data, not shown) of CP47 subunit spectra, and with PSII core spectra [1].

The lowest energy pigment(s) in isolated CP43 subunits absorb near 683 nm [43–45]. Fluorescence spectra of PSII cores obtained using 2.3 nm bandwidth 680–698 nm illumination from the lamp/monochromator system (see Materials and methods), have displayed line-narrowed vibrational sideline features (i.e. FLN) attributable to CP43 and CP47 [29]. The CP47 frequencies dominate for excitation beyond 690 nm. Excitation at 700 nm, although leading to photoconversion of the sample, gave rise to relatively little fluorescence. This result provides a further strong distinction between the strongly fluorescent inhomogeneously broadened CP47 state and the homogeneously broadened absorption extending to 730 nm.

4.3. Photoconversion as a function excitation wavelength

Although excitation of the 680–705 nm and 705–730 nm regions both give rise to significant photoconversion they exhibit profoundly different SHB activity [23,27,28]. The absence of SHB beyond 704 nm allows the use of high fluences from narrowband laser excitation to induce photoconversion *without* incurring the difficulties associated with SHB. We can associate absorption in the 705–730 nm region with PSII, as excitation here leads to Q_A^- formation in a majority of centers.

The lack of persistent SHB seen in the 705–730 nm range is sustained while up to 80% photochemical conversion of the sample is induced. This establishes that the lowest energy state of PSII is dominantly *homogeneously* broadened. This situation parallels the case for the primary donor absorption in BRCs [46,47]. If the 705–730 nm absorption in PSII were inhomogeneously broadened, photochemical SHB would occur with the same efficiency as Q_A^- formation and the fraction of the sample that could be converted to the Q_A^- state by narrowband excitation would be limited. The limiting fraction would be approximately the ratio of the SHB width to the inhomogeneous width.

In BRCs, SHB becomes observable only with excitation of zero phonon lines at the low-energy edge of the homogeneously broadened profile [47–50]. The homogeneous width of the zero phonon line was found to be consistent with the charge separation rate as measured in time domain experiments [47]. The overall bandwidth of the charge separating (P^*) state in BRCs and the lowest energy band in PSII, as determined above, are comparable at 400–500 cm⁻¹. This suggests a similar electron-phonon coupling and/or phonon frequencies.

Our experiments were performed with thin (~0.2 mm) sample cells that were immersed in superfluid helium at 1.7 K.

Experiments were performed with very low absorbed light power-densities ($\sim 5 \mu\text{W}/\text{cm}^2$ – $5 \text{ mW}/\text{cm}^2$). This eliminates the likelihood of significant *bulk* heating of the sample. Thus, any thermal activation of excited states $> 12 \text{ cm}^{-1}$ (i.e. 10 kT) higher in energy than the exciting light has a probability of $< 5 \times 10^{-5}$.

It has been noted [51] that significant transient *local* heating may persist for 26–40 ps in a (single) photosynthetic antenna complex upon absorption of a photon. This heating arises from the conversion of electronic excitation energy into (transient) vibrational excitation of the local environment. The effective local temperature rise induced by such a process was estimated to be as high as 10 degrees at 77 K [51]. In order to photo-induce charge separation in a PSII core complex that has been transiently heated by such a process, a second absorption would need to occur within the 26–40 ps period of thermal activation. The highest absorbed power densities used to induce photoconversion in this work corresponds to each PSII core complex being excited 1000 times in 600 s. The likelihood of two photons being absorbed in a single PSII core within a ~ 100 ps interval is negligible.

Estimating the lifetime of a charge-separating state to be ~ 3 ps, the FWHM of its homogeneous (Lorentzian) zero phonon line would be 1.8 cm^{-1} . The energy displacement at which excitation of such a Lorentzian profile falls to 10^{-3} of its peak value is $\sim 30 \text{ cm}^{-1}$. Thus, the fall in efficiencies seen with excitation at longer wavelengths (Fig. 5) is too gradual to be accounted for by the absorption tails of excitations at higher energy.

The possibility that the efficiency decreases seen with excitation to lower energies are due to the finite temperature of the sample and consequent absorption from a thermally activated ground state (hot-band absorption) can be excluded. Also excluded is the influence of tailing absorptions of charge-separating states to higher energy. Any such interpretation invoking these phenomena to explain lower efficiencies would also require most of the absorption in the 700–730 nm to be ‘inactive’ i.e. not leading to charge separation. This is because the ‘hot’ and the ‘tailing’ absorption would be expected to have the *same* photochemical efficiency when scaled to *absorbed* light, as the photoconversion process involves precisely the same electronic excited state.

Photoconversion efficiencies in the 690–700 nm range (Fig. 5), a range where absorption is dominated by the (inhomogeneously broadened) CP47 trap state, show efficiencies 2–5 times lower than that seen for green illumination. Some drop in yield is expected due to the selectivity of the exciting radiation. The 2.3 nm bandwidth of the excitation used in this region intercepts only CP47 absorption in a sub-population of PSII, i.e. those PSII that have CP47 trap pigments absorbing within the bandwidth of the illuminating source. This selectivity is precisely that responsible for the FLN characteristics observed in PSII [29]. Photoconversion yields from the subset of CP47 that are selectively excited are as the same as those obtained with green illumination. Additionally, the total fraction of centers that are converted exceeds the fraction of PSII whose CP47 absorption is accessible by the 2.3 nm bandwidth exciting radiation. We can conclude that excitation of either the inho-

mogeneously broadened CP47 trap or of the homogeneously broadened underlying state when excited at wavelengths above 700 nm both lead to efficient photoconversion.

4.4. Assignment of the lowest energy excitation in PSII cores

The homogeneously broadened absorption extending to 730 nm in PSII is the lowest-energy optically accessible electronic excitation of the reaction center of oxygen evolving PSII core complexes. Excitation at wavelengths to 728 nm leads to accumulation of the charge-separated Q_A^- configuration. Excitation fluences available at 725 nm led to photoconversion of $\sim 30\%$ of PSII centers without reaching saturation. The spectral profile of the *change* in intensity of the low energy tail is similar to that of the tail itself and is independent of excitation wavelength to within experimental error. As excitation at 704 nm achieves 80% photoconversion of PSII, the 700–730 nm tail can be associated with a *majority* of PSII centers.

Radiationless deactivation of electronic excitations of the charge-separating pigment assembly (P680) to the lowest electronic and vibrational levels of this assembly can be expected to be extremely rapid [47]. Charge separation would then be expected to ensue from the *lowest electronic excited state* of the system. Thus, charge separation yields when corrected for absorbance could be expected to be independent of the excitation wavelength.

We have seen that the photochemical yields of the charge-separated Q_A^- configuration drop very significantly with excitation beyond 700 nm. This observation provides a significant challenge to any assignment of the lowest-energy excitation of PSII. We consider two possible assignments of the low-energy state that address this and other key characteristics of the absorption. Our first suggestion assigns the low-energy state as a weak, low-energy exciton component of the ‘special pair’, which are the closely coupled reaction center pigments P_{D1} and P_{D2} . Secondly, we consider the low-energy state as arising from the direct optical excitation to a charge-separated state of $\text{P}_{\text{D1}}-\text{P}_{\text{D2}}$.

4.4.1. The sandwich-coupled model with slow vibrational relaxation

Our first model is suggested by analogies of the low energy absorption in PSII with the charge separating (P^*) state in BRCs. This well-studied and characteristic excitation in BRCs is homogeneously broadened, having a width comparable to that indicated by our fit of the 705 nm band in PSII. The lowest energy band in PSII has a dipole strength estimated to be $0.15 \pm 0.05 \text{ chl } a$ when modelled as a Gaussian (Fig. 3). The assignment of this as a pigment excitation with $< 1 \text{ chl } a$ dipole strength immediately predicates the existence of exciton coupling within the photo-active pigment assembly of PSII comparable to or greater than the linewidth of the band ($\sim 500 \text{ cm}^{-1}$). A splitting of this magnitude is consistent with the ‘special pair’ distance of 7.6 Å recently reported [2] in PSII. This value is almost identical to the equivalent distances in BRCs [52].

However, a *weakly* absorbing lowest-energy exciton component is precisely the opposite of what is seen in BRCs. This

reversal would require an interaction between transition dipoles in a sandwich configuration [19,53]. The orientation of the P_{D1} and P_{D2} chl *a* molecules in PSII are known [2–6] and the directions of their transition dipoles, as inferred from the dipole directions in isolated chl *a* [54], have an ‘in line’ orientation. The existence of a ‘sandwich pair’ of transition dipoles would indicate exceptional protein-induced changes of the electronic characteristics of the P_{D1} and P_{D2} chl *a* molecules in PSII. The higher-energy exciton partner of the charge-separating state in BRC is inferred to be narrow [55] and in this respect the 683.5 nm feature in PSII plant cores, which we have associated with P680, exhibits the same characteristics.

Within this picture, transient absorption changes reported for PSII cores [56] near 680 nm upon 10 ps laser excitation would not correspond to the bleach of a lower-energy charge-separating state. This bleach would then be associated with changes in more intense component(s) of a strongly exciton-coupled photo-active P680 assembly where coupling is dominated by the P_{D1} – P_{D2} interaction. The energy separation between the narrow 683.5 nm feature that we have associated with P680 and the peak of the homogeneously broadened low energy state at 705 nm is 445 cm^{-1} which corresponds to 2.2 kT at ambient temperatures.

In order to account for the low yields of photoconversion seen with long wavelength excitation, we need to further propose that only vibrationally-excited states contribute significantly to the overall charge separation process. This is in contrast to the situation in the BRCs where the electronic origin and vibrationally excited levels charge separate at the same rate [47,57]. Jortner has suggested [58] a process, schematically represented in Fig. 6, in which vibrationally (localized phonon) excited levels of the charge-separating state, i.e. those energetically closer to a crossing to the putative charge-separated state, charge separate more rapidly than levels at lower energy. If vibrational relaxation is relatively slow, charge separation yields may increase with excitation at higher energy.

4.4.2. The redox tunable charge transfer trap model

Charge separated configurations of PSII such as $P680^+ - Pheo_{D1}^-$, are not considered to be optically accessible. Direct optical excitation of such ‘dark’ electronic states of the system is strongly inhibited by both [17] the lack of electronic overlap between donor (D) and acceptor (A) pigments and also by low Franck–Condon factors involved in passing from $D-A$ to $D^+ - A^-$. The equilibrium geometries of D and D^+ , A and A^- will in general be significantly displaced, i.e., cations and anions are inherently smaller and bigger respectively, than their parents. Consequently, vibrational overlap factors between the respective D/D^+ and A/A^- configurations become minimal.

We again take inspiration from studies of BRCs that have shown that the ‘special pair’ of bacterio-chlorophylls are close enough to allow significant electronic overlap. The characteristic *homogeneous* broadening of the charge-separating state of BRCs has been attributed to [59,60] a ~10% mixing of a charge-separated state with the pigment excitation. This is enabled by the electronic overlap in the ‘special pair’. The unusual and marked *blue* shift of the peak maximum of the P band in *R. Sphaeroides* with increasing temperature has also been recently explained in

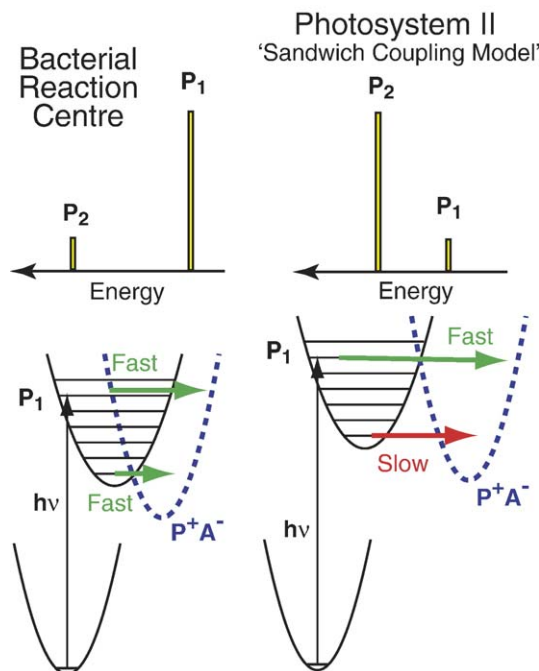


Fig. 6. Schematic comparison of exciton levels of the strongly coupled, ‘in line’, coupling of the ‘special pair’ in BRC’s (left), and the ‘sandwich’ coupling model of PSII which leads to an anomalously *low* intensity P_1 state (right). Also shown are potential surfaces of exciton and charge separated states, consistent with a dominance of crossing to the charge-separated state from vibrationally excited levels of the P_1 state of PSII. Within this model, this process is competitive with vibrational relaxation, leading to the higher yields of photoconversion seen with direct excitation of higher vibrational levels (see text).

terms of a vibronic coupling model, dynamically mixing exciton-coupled dimer states and charge transfer excitations [61].

When charge transfer character is induced in pigment excitations, as evidenced by homogeneous broadening and large Stark effects of the P band, the mixing responsible for this will also transfer a corresponding pigment excitation character to the charge transfer state. Thus, to the extent to which the systems are mixed (10% in BRCs) the nominally ‘dark’ charge transfer state can gain optical intensity from pigment excitations. Other properties of the state such as the excitation energy remain identifiable as a (90%) charge transfer excitation. As it has now been established that the P_{D1} – P_{D2} distance in PSII is indeed the same as the corresponding distance in BRCs [2], it is appropriate to invoke the possibility of a similar electronic overlap between the chl *a* molecules of the ‘special pair’ in PSII. Transient absorption and fluorescence studies of D1/D2/cyt b_{559} particles have been analysed within a model [9] in which intensity is transferred between exciton levels and charge transfer states of P_{D1} – P_{D2} . However, in D1/D2/cyt b_{559} particles there is no equivalent low energy absorption to that seen in our PSII core preparations.

This line of argument suggests an assignment of the 705 nm band in PSII as a charge transfer excitation of the ‘special pair’ (Fig. 7). This state could be $(P_{D1}^+ - P_{D2}^-)$, $(P_{D1}^- - P_{D2}^+)$, or a corresponding delocalised combination, $(P_{D1}^+ - P_{D2}^-) \pm (P_{D1}^- - P_{D2}^+)$. Its absorption strength, corresponding to 0.15 chl *a*, would then be attributed to its chl *a* Q_y character. This absorption strength is clearly compatible with estimates of the mixing in BRCs.

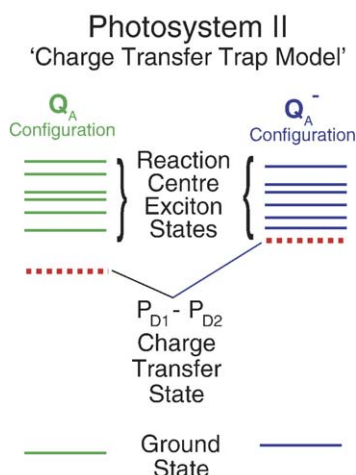


Fig. 7. Schematic of the eigenstates of the reaction center PSII within the charge-transfer trap model. The electrochromic fields experienced upon creation of the metastable Q_A^- configuration lead to relatively small changes in the exciton-coupled levels of the reaction center chlorin Q_y excitations but induce a strong blue shift the optically accessible inter-chlorin $P_{D1}-P_{D2}$ charge transfer excitation (see text).

In order to account for the reduced yields of photoconversion with long wavelength excitation, we further suggest that excitation of a 'pure' $P_{D1}-P_{D2}$ charge-transfer state that generates the corresponding radical pair is not effective in photoconverting a PSII sample. Efficient and long-lived charge separation, forming $P680^+-Pheo_{D1}^-$, requires charge separation originating from the other (active branch accessory) chl *a* within the reaction center and correspondingly generates other radical pairs. This is in line with some current models [9,62]. However, exciton coupling between the central chlorins will ensure eigenstates of the system involving $P_{D1}-P_{D2}$ basis excitations will be mixed with basis states localized on other chlorins. This mixing of nominally $P_{D1}-P_{D2}$ excitations with those of other central chlorins may lead to the reduced but non-zero efficiency of photoconversion when exciting in the 700–730 nm region.

The assignment of the 705 nm band as a charge transfer excitation of $P_{D1}-P_{D2}$ makes it far easier to account for the marked reduction in its absorption intensity when the sample is converted to the metastable charge-separated Q_A^- configuration. A charge-transfer state is strongly affected by local charges, and may show extremely large electrochromic effects. The reduction of Q_A , along with the oxidation of a secondary donor induces significant electrochromic effects on chlorin excitations and far larger effects may be expected for charge transfer states. In D2/D2/cyt_b₅₅₉ particles, this charge transfer state may be at a quite different energy [9]. In order to account for the reduction of intensity of the $P_{D1}-P_{D2}$ charge transfer state upon photoconversion, an increase of the energy of this state by half the linewidth (250 cm⁻¹ or 30 meV) could account for the apparent ~2-fold reduction in intensity of the band. A shift of the band to higher energy and towards the CP47 excitation would lead to the remaining exposed tail having half the intensity at 705 nm. The remaining tail would then have a slightly different shape to that originally, with more intensity at 705 nm than at longer wavelengths. The precision available in our data would not entirely exclude this possibility.

Strong electrochromism of a $P_{D1}-P_{D2}$ charge transfer excitation could serve as a redox tunable trap, being both the lowest energy excitation of PSII and particularly sensitive to the charge state of nearby redox active co-factors.

4.5. Comparing the models

Neither model presented immediately accounts for all the properties reported for the lowest energy absorption. A strong electrochromic shift to higher energy of a $P_{D1}-P_{D2}$ charge transfer state upon photoconversion could lead to a reduction of absorption in the tail region but would also imply some shape change in the remaining absorption. It is hard to see how a low energy 'sandwich' exciton component could exhibit a dramatic change in intensity upon Q_A^- formation. One would need to invoke dramatic changes in exciton couplings driven by electrochromic shifts of pigment excitations.

The gradual drop in yields seen (Fig. 5) for a given absorbed fluence beyond 700 nm could be accounted for by a slowly vibrationally-relaxing manifold intercepting with a charge separated state, following the model proposed by Jortner [58]. However, there is no experimental or theoretical evidence for either the 'sandwich' exciton-coupling in $P_{D1}-P_{D2}$ nor evidence for slow (>10 ps) vibrational relaxation. In the redox-tunable charge-transfer trap model, the reduction of efficiency suffered by excitation into such a state is attributed to its predominant $P_{D1}-P_{D2}$ character and the ineffectiveness of the resultant radical pair in forming a stable charge-separated configuration. It is, however, more difficult to see why this yield varies significantly between 700 nm and 730 nm as the same electronic excited state is nominally being created.

One way of approaching this latter difficulty is via our ability to dissect the overall yield versus absorbed photons curve of PSII (Fig. 5) into comparable fractions having QEs of 0.7, 0.05 and 0.03. If each PSII fraction was initially poised in a somewhat different configuration with respect to some redox co-factors, the energy of its $P_{D1}-P_{D2}$ charge transfer band may be significantly different. The 700–730 nm tail may be composite of charge-transfer absorptions of these fractions. At each wavelength, the proportion of each fraction may be somewhat different. For example, excitation at longer wavelengths appears to selectively excite lower efficiency fractions of PSII. Within this idea, PSII may use the redox tuning of the charge-transfer trap depth to control charge separation yields.

5. Conclusions

The unexpected and unusual characteristics of the lowest energy state of PSII in spinach may be a significant element in the overall process of oxygenic photosynthesis. The prospect of a redox-tunable trap in PSII is particularly intriguing. A recent report [63] of PSII activity of sunflower and bean plants at ambient temperatures utilizing excitation wavelengths as long as 780 nm may be connected with our ability to induce charge separation at 1.7 K in PSII with wavelengths as long as 730 nm. Studies on PSII sourced from other organisms, particularly cyanobacteria, may help determine the generality of the phenomenon

and help distinguish between possible assignments of state(s) absorbing in the deep red. Our preliminary measurements on highly active *Thermosynechococcus elongatus* PSII cores have also shown significant 'C550' electrochromism induced by light beyond 700 nm.

The detection of emission from the lowest energy state of PSII, frustrated in plant PSII samples [31], may be possible in cyanobacteria as excitation of PSI contaminants can in principle be avoided. SHB processes may become measurable near 730 nm in optically dense samples with the development of more sensitive spectral-hole readout techniques. Such measurements would provide valuable information regarding the nature of the excited-state, and such studies are currently being planned. The ability to selectively excite and characterize the lowest-energy reaction center state of intact PSII cores without interference from absorption of the proximal antennae may also be useful in studying primary processes in PSII with pump-probe and single particle techniques.

Acknowledgements

EK would like to acknowledge a particularly useful discussion with Professor M. Collins. We would also like to acknowledge discussion with Dr. W. Rutherford and Dr. R. Steffen as well as Dr. R. Steffen for assistance with the fitting of photochemical yield data.

References

- [1] P.J. Smith, S. Peterson, V.M. Masters, T. Wydrzynski, S. Styring, E. Krausz, R.J. Pace, Magneto-optical measurements of the pigments in fully active photosystem II core complexes from plants, *Biochemistry* 41 (2002) 1981–1989.
- [2] B. Loll, J. Kern, W. Saenger, A. Zouni, J. Biesiadka, Towards complete cofactor arrangement in the 3.0 Å resolution crystal structure of photosystem II, *Nature* 438 (2005) 1040–1044.
- [3] A. Zouni, H.T. Witt, J. Kern, P. Fromme, N. Krauss, W. Saenger, P. Orth, Crystal structure of photosystem II from *Synechococcus elongatus* at 3.8 Å resolution, *Nature* 409 (2001) 739–743.
- [4] N. Kamiya, J.-R. Shen, Crystal Structure Analysis of Photosystem II from *Thermosynechococcus vulcanus*, in: PS2001: 12th International Congress of Photosynthesis Brisbane, Australia, 2001, p. S5-002.
- [5] N. Kamiya, J.-R. Shen, Crystal structure of oxygen-evolving photosystem II from *Thermosynechococcus vulcanus* at 3.7-Å resolution, *Proc. Natl. Acad. Sci. U. S. A.* 100 (2003) 98–103.
- [6] K.N. Ferreira, T.M. Iverson, K. Maghlaoui, J. Barber, S. Iwata, Architecture of the photosynthetic oxygen-evolving center, *Science* 303 (2004) 1831–1838.
- [7] M. Seibert, Biochemical, biophysical, and structural characterization of the isolated photosystem II reaction center complex, in: J. Deisenhofer, J. Norris (Eds.), *The Photosynthetic Reaction Center*, vol. 1, Academic Press, New York, 1993, pp. 319–356.
- [8] R.N. Frese, M. Germano, F.L. de Weerd, I.H.M. van Stokkum, A.Y. Shkuropatov, V.A. Shuvalov, H.J. van Gorkom, R. van Grondelle, J.P. Dekker, Electric field effects on the chlorophylls, pheophytins, and β -carotenes in the reaction center of photosystem II, *Biochemistry* 42 (2003) 9205–9213.
- [9] V.L. Novoderezhkin, E.G. Andrizhiyevskaya, J.P. Dekker, R. van Grondelle, Pathways and timescales of primary charge separation in the photosystem II reaction center as resolved by a simultaneous fit of time-resolved fluorescence and transient absorption, *Biophys. J.* 89 (2005) 1464–1481.
- [10] M.-L. Groot, F. van Mourik, C. Eijkelhoff, I.H.M. van Stokkum, J.P. Dekker, R. van Grondelle, Charge separation in the reaction center of photosystem II studied as a function of temperature, *Proc. Natl. Acad. Sci. U. S. A.* 94 (1997) 4389–4394.
- [11] V.I. Prokhorenko, A.R. Holzwarth, Primary processes and structure of the photosystem II reaction center: a photon echo study, *J. Phys. Chem., B* 104 (2000) 11563–11578.
- [12] M.G. Müller, M. Hücke, M. Reus, A.R. Holzwarth, Annihilation processes in the isolated D1–D2-cyt-b559 reaction center complex of photosystem II. An intensity-dependence study of femtosecond transient absorption, *J. Phys. Chem.* 100 (1996) 9537–9544.
- [13] G. Raszewski, W. Saenger, T. Renger, Theory of optical spectra of photosystem II reaction centers: location of the triplet state and the identity of the primary electron donor, *Biophys. J.* 88 (2005) 986–998.
- [14] L.M. Yoder, A.G. Cole, R.J. Sension, Structure and function in the isolated reaction center complex of photosystem II: energy and charge transfer dynamics and mechanism, *Photosynth. Res.* 72 (2002) 147–158.
- [15] B.A. Diner, F. Rappaport, Structure, dynamics, and energetics of the primary photochemistry of photosystem II of oxygenic photosynthesis, *Annu. Rev. Plant Biol.* 53 (2002) 551–580.
- [16] J.P. Dekker, R. van Grondelle, Primary charge separation in photosystem II, *Photosynth. Res.* 63 (2000) 195–208.
- [17] G. Renger, A.R. Holzwarth, Primary electron transfer, in: T.J. Wydrzynski, K. Satoh (Eds.), *Photosystem II — The Light-Driven Water:Plastoquinone Oxidoreductase*, *Adv. Photosynth. Respir.*, vol. 22, Springer, Dordrecht, The Netherlands, 2005, pp. 139–175.
- [18] S. Peterson Årsköld, B.J. Prince, E. Krausz, P.J. Smith, R.J. Pace, R. Picorel, M. Seibert, Low-temperature spectroscopy of fully active PSII cores. Comparisons with CP43, CP47, D1/D2/cyt b559 fragments, *J. Lumin.* 108 (2004) 97–100.
- [19] J.L. Hughes, B.J. Prince, S.P. Årsköld, P.J. Smith, R.J. Pace, H. Riesen, E. Krausz, The native reaction centre of photosystem II: a new paradigm for P680, *Aust. J. Chem.* 57 (2004) 1179–1183.
- [20] E. Krausz, J.L. Hughes, P. Smith, R. Pace, S. Peterson Årsköld, Oxygen-evolving photosystem II core complexes: a new paradigm based on the spectral identification of the charge-separating state, the primary acceptor and assignment of low-temperature fluorescence, *Photochem. Photobiol. Sci.* 4 (2005) 744–753.
- [21] S. Peterson Årsköld, P.J. Smith, J.-R. Shen, R.J. Pace, E. Krausz, Key cofactors of photosystem II cores from four organisms identified by 1.7-K absorption, CD, and MCD, *Photosynth. Res.* 84 (2005) 309–316.
- [22] S. Peterson Årsköld, V.M. Masters, B.J. Prince, P.J. Smith, R.J. Pace, E. Krausz, Optical spectra of *Synechocystis* and spinach photosystem II preparations: identification of the D1-pheophytin energies and stark shifts, *J. Am. Chem. Soc.* 125 (2003) 13063–13074.
- [23] J.L. Hughes, B.J. Prince, E. Krausz, P.J. Smith, R.J. Pace, H. Riesen, Highly efficient spectral hole-burning in oxygen-evolving photosystem II preparations, *J. Phys. Chem., B* 108 (2004) 10428–10439.
- [24] J.L. Hughes, E. Krausz, P.J. Smith, R.J. Pace, The lowest-energy excited state of P680 in oxygen-evolving photosystem II extends to 700 nm, in: A. van der Est, D. Bruce (Eds.), *PS2004: 13th International Congress of Photosynthesis*, Montreal, Canada, 2004, pp. S3–S6.
- [25] W.L. Butler, Primary photochemistry of photosystem II of photosynthesis, *Acc. Chem. Res.* 6 (1973) 177–184.
- [26] D.B. Knaff, D.L. Arnon, Spectral evidence for a new photoreactive component of the oxygen-evolving system in photosynthesis, *Proc. Natl. Acad. Sci. U. S. A.* 63 (1969) 963–969.
- [27] J.L. Hughes, E. Krausz, P.J. Smith, R.J. Pace, H. Riesen, Probing the lowest energy chlorophyll a states of photosystem II via selective spectroscopy: new insights on P680, *Photosynth. Res.* 84 (2005) 93–98.
- [28] J.L. Hughes, P.J. Smith, R.J. Pace, E. Krausz, Spectral hole-burning at the low-energy absorption edge of photosystem II core complexes, *J. Lumin.* 119–120 (2006) 298–303.
- [29] E. Krausz, J.L. Hughes, P.J. Smith, R.J. Pace, S. Peterson Årsköld, Assignment of the low-temperature fluorescence in oxygen-evolving photosystem II, *Photosynth. Res.* 84 (2005) 193–199.
- [30] E.G. Andrizhiyevskaya, A. Chojnicka, J.A. Bautista, B.A. Diner, R. van Grondelle, J.P. Dekker, Origin of the F685 and F695 fluorescence in photosystem II, *Photosynth. Res.* 84 (2005) 173–180.

- [31] J.L. Hughes, P.J. Smith, R.J. Pace, E. Krausz, Low energy absorption and luminescence of higher plant photosystem II core samples, *J. Lumin.* (2006), doi:10.1016/j.jlumin.2006.01.142.
- [32] K. Riley, R. Jankowiak, M. Rätsep, G.J. Small, V. Zazubovich, Evidence for highly dispersive primary charge separation kinetics and gross heterogeneity in the isolated PSII reaction center of green plants, *J. Phys. Chem., B* 108 (2004) 10346–10356.
- [33] B. Hillmann, E. Schlodder, Electron transfer reactions in photosystem II core complexes from *Synechococcus* at low temperature-difference spectrum of P680⁺Q_A⁻/P680Q_A at 77 K, *Biochim. Biophys. Acta* 1231 (1995) 76–88.
- [34] C. Zhang, A. Boussac, A.W. Rutherford, Low-temperature electron transfer in photosystem II: a tyrosyl radical and semiquinone charge pair, *Biochemistry* 43 (2004) 13787–13795.
- [35] C.A. Tracewell, G.W. Brudvig, Two redox-active β -carotene molecules in photosystem II, *Biochemistry* 42 (2003) 9127–9136.
- [36] J.H.A. Nugent, I.P. Muhiuddin, M.C. Evans, Electron transfer from the water oxidizing complex at cryogenic temperatures: the S₁ to S₂ step, *Biochemistry* 41 (2002) 4117–4126.
- [37] J. Hanley, Y. Deligiannakis, A. Pascal, P. Faller, A.W. Rutherford, Carotenoid oxidation in photosystem II, *Biochemistry* 38 (1999) 8189–8195.
- [38] P. Faller, A.W. Rutherford, R.J. Debus, Tyrosine D oxidation at cryogenic temperature in photosystem II, *Biochemistry* 41 (2002) 12914–12920.
- [39] N. Getoff, Pulse radiolysis studies of β -carotene in oxygenated DMSO solution. Formation of β -carotene radical cation, *Radiat. Res.* 154 (2000) 692–696.
- [40] F.T.H. den Hartog, J.P. Dekker, R. van Grondelle, S. Völker, Spectral distributions of “Trap” pigments in the RC, CP47, and CP47-RC complexes of photosystem II at low temperature: a fluorescence line-narrowing and hole-burning study, *J. Phys. Chem., B* 102 (1998) 11007–11016.
- [41] H.C. Chang, R. Jankowiak, C.F. Yocum, R. Picorel, M. Alfonso, M. Seibert, G.J. Small, Exciton level structure and dynamics in the CP47 antenna complex of photosystem II, *J. Phys. Chem.* 98 (1994) 7717–7724.
- [42] F.L. de Weerd, M.A. Palacios, E.G. Andrizhiyevskaya, J.P. Dekker, R. van Grondelle, Identifying the lowest electronic states of the chlorophylls in the CP47 core antenna protein of photosystem II, *Biochemistry* 41 (2002) 15224–15233.
- [43] M.-L. Groot, R.N. Frese, F.L. de Weerd, K. Bromek, A. Pettersson, Spectroscopic properties of the CP43 core antenna protein of photosystem II, *Biophys. J.* 77 (1999) 3328–3340.
- [44] J.L. Hughes, B.J. Prince, S. Peterson Årsköld, E. Krausz, R.J. Pace, R. Picorel, M. Seibert, Photo-conversion of chlorophylls in higher-plant CP43 characterized by persistent spectral hole-burning at 1.7 K, *J. Lumin.* 108 (2004) 131–136.
- [45] R. Jankowiak, V. Zazubovich, M. Rätsep, S. Matsuzaki, M. Alfonso, R. Picorel, M. Seibert, G.J. Small, The CP43 core antenna complex of photosystem II possesses two quasi-degenerate and weakly coupled Q_y-Trap States, *J. Phys. Chem., B* 104 (2000) 11805–11815.
- [46] S.G. Boxer, Photosynthetic reaction center spectroscopy and electron transfer dynamics in applied electric fields, in: J. Deisenhofer, J.R. Norris (Eds.), *The Photosynthetic Reaction Center*, vol. II, Academic Press, San Diego, 1993, pp. 179–220.
- [47] T.R. Middendorf, L.T. Mazzola, D.F. Gaul, C.C. Schenck, S.G. Boxer, Photochemical hole-burning spectroscopy of a photosynthetic reaction center mutant with altered charge separation kinetics: properties and decay of the initially excited state, *J. Phys. Chem., B* 95 (1991) 10142–10151.
- [48] N.R.S. Reddy, P.A. Lyle, G.J. Small, Applications of spectral hole burning spectroscopies to antenna and reaction center complexes, *Photosynth. Res.* 31 (1992) 167–194.
- [49] N.R.S. Reddy, S.V. Kolaczowski, G.J. Small, Nonphotochemical hole burning of the reaction center of *Rhodospseudomonas viridis*, *J. Phys. Chem.* 97 (1993) 6934–6940.
- [50] N.R.S. Reddy, S.V. Kolaczowski, G.J. Small, A photoinduced persistent structural transformation of the special pair of a bacterial reaction center, *Science* 260 (1993) 68–71.
- [51] L. Valkunas, V. Gulbinas, Nonlinear exciton annihilation and local heating effects in photosynthetic antenna systems, *Photochem. Photobiol.* 66 (1997) 628–634.
- [52] R.E. Blankenship, *Molecular Mechanisms of Photosynthesis*, Blackwell Science, Oxford, 2002.
- [53] C.R. Cantor, P.R. Schimmel, Part II: Techniques for the Study of Biological Structure and Function, W. H. Freeman and Company, San Francisco, 1980.
- [54] M.A.M.J. van Zandvoort, D. Wróbel, P. Lettinga, G. van Ginkel, Y.K. Levine, The orientation of the transition dipole moments of chlorophyll a and pheophytin a in their molecular frame, *Photochem. Photobiol.* 62 (1995) 299–308.
- [55] T. Mar, G. Gingras, Origin of optical activity in the purple bacterial reaction center, *Biochemistry* 34 (1995) 9071–9078.
- [56] J.P.M. Schelvis, M. Germano, T.J. Aartsma, H.J. van Gorkom, Energy transfer and trapping in photosystem II core particles with closed reaction centres, *Biochim. Biophys. Acta* 1230 (1995) 165–169.
- [57] N.R.S. Reddy, R. Picorel, G.J. Small, B896 and B870 components of the *Rhodobacter sphaeroides* antenna: a hole burning study, *J. Phys. Chem.* 96 (1992) 6458–6464.
- [58] J. Jortner, Dynamics of the primary events in bacterial photosynthesis, *J. Am. Chem. Soc.* 102 (1980) 6676–6686.
- [59] A. Warshel, W.W. Parson, Spectroscopic properties of photosynthetic reaction centres. 1. Theory, *J. Am. Chem. Soc.* 109 (1987) 6143–6152.
- [60] W.W. Parson, A. Warshel, Spectroscopic properties of photosynthetic reaction centres. 2. Application of the theory to *Rhodospseudomonas viridis*, *J. Am. Chem. Soc.* 109 (1987) 6152–6163.
- [61] T. Renger, Theory of optical spectra involving charge transfer states: dynamic localization predicts a temperature dependent optical band shift, *Phys. Rev. Lett.* 93 (2004) 188101–188104.
- [62] Y. Miloslavina, M. Szczepaniak, M.G. Müller, J. Sander, M. Nowaczyk, M. Rögner, A.R. Holzwarth, Charge separation kinetics in intact photosystem II core particles is trap-limited. A picosecond fluorescence study, *Biochemistry* 45 (2006) 2436–2442.
- [63] H. Pettai, V. Oja, A. Freiberg, A. Laik, Photosynthetic activity of far-red light in green plants, *Biochim. Biophys. Acta* 1708 (2005) 311–321.